

First observation of the decay $\tau^- \rightarrow \phi K^- \nu_\tau$

Belle Collaboration

K. Inami^{t,*}, K. Abe^g, K. Abe^{am}, I. Adachi^g, H. Aihara^{ao}, D. Anipko^a, K. Arinstein^a,
V. Aulchenko^a, T. Aushev^{p,k}, S. Bahinipati^c, A.M. Bakich^{aj}, E. Barberio^s, M. Barbero^f, I. Bedny^a,
I. Bizjak^l, A. Bondar^a, A. Bozek^x, M. Bračko^{g,r,l}, T.E. Browder^f, A. Chen^v, K.-F. Chen^w,
W.T. Chen^v, R. Chistov^k, Y. Choi^{ai}, Y.K. Choi^{ai}, J. Dalseno^s, M. Danilov^k, A. Drutskoy^c,
S. Eidelman^a, D. Epifanov^a, S. Fratina^l, N. Gabyshev^a, T. Gershon^g, G. Gokhroo^{ak}, H. Haⁿ,
J. Haba^g, K. Hara^t, K. Hayasaka^t, H. Hayashii^u, M. Hazumi^g, D. Heffernan^{ac}, T. Hokuue^t,
Y. Hoshi^{am}, S. Hou^v, W.-S. Hou^w, Y.B. Hsiung^w, T. Iijima^t, A. Ishikawa^{ao}, R. Itoh^g, Y. Iwasaki^g,
J.H. Kang^{at}, P. Kapusta^x, S.U. Kataoka^u, H. Kawai^b, T. Kawasaki^z, H.R. Khan^{ap}, H. Kichimi^g,
Y.J. Kim^d, S. Korpar^{r,l}, P. Križan^{q,l}, P. Krokovny^g, R. Kulasiri^c, R. Kumar^{ad}, A. Kuzmin^a,
Y.-J. Kwon^{at}, G. Leder^j, T. Lesiak^x, S.-W. Lin^w, D. Liventsev^k, G. Majumder^{ak}, F. Mandl^j,
T. Matsumoto^{aq}, A. Matyja^x, S. McOnie^{aj}, W. Mitaroff^j, H. Miyake^{ac}, H. Miyata^z, Y. Miyazaki^t,
R. Mizuk^k, J. Mueller^{af}, Y. Nagasaka^h, I. Nakamura^g, E. Nakano^{ab}, M. Nakao^g, S. Nishida^g,
O. Nitoh^{ar}, S. Ogawa^{al}, T. Ohshima^t, S. Okuno^m, Y. Onuki^{ag}, H. Ozaki^g, H. Palka^x, C.W. Park^{ai},
H. Park^o, L.S. Peak^{aj}, L.E Piilonen^{as}, A. Poluektov^a, Y. Sakai^g, T. Schietinger^p, O. Schneider^p,
A.J. Schwartz^c, R. Seidl^{i,ag}, K. Senyo^t, M.E. Sevier^s, H. Shibuya^{al}, B. Shwartz^a, V. Sidorov^a,
J.B. Singh^{ad}, A. Somov^c, N. Soni^{ad}, S. Stanič^{aa}, M. Starič^l, H. Stoeck^{aj}, S.Y. Suzuki^g, O. Tajima^g,
N. Tamura^z, M. Tanaka^g, G.N. Taylor^s, Y. Teramoto^{ab}, X.C. Tian^{ae}, T. Tsukamoto^g, S. Uehara^g,
K. Ueno^w, T. Uglov^k, S. Uno^g, P. Urquijo^s, Y. Usov^a, G. Varner^f, S. Villa^p, E. Wonⁿ, C.-H. Wu^w,
B.D. Yabsley^{aj}, A. Yamaguchi^{an}, Y. Yamashita^y, L.M. Zhang^{ah}, V. Zhilich^a, A. Zupanc^l

^a Budker Institute of Nuclear Physics, Novosibirsk, Russia

^b Chiba University, Chiba, Japan

^c University of Cincinnati, Cincinnati, OH, USA

^d The Graduate University for Advanced Studies, Hayama, Japan

^e Gyeongsang National University, Chinju, South Korea

^f University of Hawaii, Honolulu, HI, USA

^g High Energy Accelerator Research Organization (KEK), Tsukuba, Japan

^h Hiroshima Institute of Technology, Hiroshima, Japan

ⁱ University of Illinois at Urbana-Champaign, Urbana, IL, USA

^j Institute of High Energy Physics, Vienna, Austria

^k Institute for Theoretical and Experimental Physics, Moscow, Russia

^l J. Stefan Institute, Ljubljana, Slovenia

^m Kanagawa University, Yokohama, Japan

ⁿ Korea University, Seoul, South Korea

^o Kyungpook National University, Taegu, South Korea

^p Swiss Federal Institute of Technology of Lausanne, EPFL, Lausanne, Switzerland

^q University of Ljubljana, Ljubljana, Slovenia

^r University of Maribor, Maribor, Slovenia

^s University of Melbourne, Victoria, Australia

^t Nagoya University, Nagoya, Japan

^u Nara Women's University, Nara, Japan

^v National Central University, Chung-li, Taiwan

- ^w Department of Physics, National Taiwan University, Taipei, Taiwan
^x H. Niewodniczanski Institute of Nuclear Physics, Krakow, Poland
^y Nippon Dental University, Niigata, Japan
^z Niigata University, Niigata, Japan
^{aa} University of Nova Gorica, Nova Gorica, Slovenia
^{ab} Osaka City University, Osaka, Japan
^{ac} Osaka University, Osaka, Japan
^{ad} Panjab University, Chandigarh, India
^{ae} Peking University, Beijing, PR China
^{af} University of Pittsburgh, Pittsburgh, PA, USA
^{ag} RIKEN BNL Research Center, Brookhaven, NY, USA
^{ah} University of Science and Technology of China, Hefei, PR China
^{ai} Sungkyunkwan University, Suwon, South Korea
^{aj} University of Sydney, Sydney, NSW, Australia
^{ak} Tata Institute of Fundamental Research, Bombay, India
^{al} Toho University, Funabashi, Japan
^{am} Tohoku Gakuin University, Tagajo, Japan
^{an} Tohoku University, Sendai, Japan
^{ao} Department of Physics, University of Tokyo, Tokyo, Japan
^{ap} Tokyo Institute of Technology, Tokyo, Japan
^{aq} Tokyo Metropolitan University, Tokyo, Japan
^{ar} Tokyo University of Agriculture and Technology, Tokyo, Japan
^{as} Virginia Polytechnic Institute and State University, Blacksburg, VA, USA
^{at} Yonsei University, Seoul, South Korea

Received 10 September 2006; received in revised form 2 October 2006; accepted 19 October 2006

Available online 27 October 2006

Editor: M. Doser

Abstract

We present the first observation of τ lepton decays to hadronic final states with a ϕ -meson. This analysis is based on 401 fb^{-1} of data accumulated at the Belle experiment. The branching fraction obtained is $\mathcal{B}(\tau^- \rightarrow \phi K^- \nu_\tau) = (4.05 \pm 0.25 \pm 0.26) \times 10^{-5}$.

© 2006 Elsevier B.V. All rights reserved.

PACS: 13.35.Dx; 14.40.Cs

Keywords: Tau; Phi

1. Introduction

Hadronic τ decays with a ϕ -meson in the final state are valuable to investigate QCD at a low mass scale. However, they have never been observed due to their small branching fractions. The decay $\tau^- \rightarrow \phi K^- \nu_\tau$ is Cabibbo-suppressed and further restricted by its small phase space, while the decay $\tau^- \rightarrow \phi \pi^- \nu_\tau$ is suppressed by the OZI rule although it is Cabibbo-allowed (Fig. 1). The branching fraction of the former can roughly be estimated by scaling the analogous Cabibbo-allowed decay $\tau^- \rightarrow K^* K^- \nu_\tau$ [1] by $\tan^2 \theta_c$ and the ratio of the phase space of the two decays, resulting in $\mathcal{B}(\tau^- \rightarrow \phi K^- \nu_\tau) \sim 2 \times 10^{-5}$. Similarly, the vector dominance model predicts $\mathcal{B}(\tau^- \rightarrow \phi \pi^- \nu_\tau) = (1.20 \pm 0.48) \times 10^{-5}$ [2], whereas the CVC upper limit following from the cross section for $e^+ e^- \rightarrow \phi \pi^0$ is $\mathcal{B}(\tau^- \rightarrow \phi \pi^- \nu_\tau) < 3 \times 10^{-4}$ at the 90% confidence level [3].

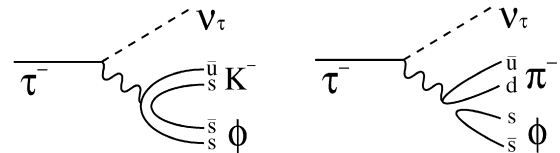


Fig. 1. Diagrams for $\tau^- \rightarrow \phi K^- \nu_\tau$ (left) and $\tau^- \rightarrow \phi \pi^- \nu_\tau$ (right).

Previously, the CLEO Collaboration searched for these decays using 3.1 fb^{-1} of data taken on the $\Upsilon(4S)$ resonance. They set upper limits of $\mathcal{B}(\tau^- \rightarrow \phi K^- \nu_\tau) < (5.4\text{--}6.7) \times 10^{-5}$ and $\mathcal{B}(\tau^- \rightarrow \phi \pi^- \nu_\tau) < (1.2\text{--}2.0) \times 10^{-4}$ at the 90% confidence level, depending on the mechanism assumed for the decay [4]. Here we report the first measurement of the $\tau^- \rightarrow \phi K^- \nu_\tau$ decay. (Throughout this Letter charge-conjugate states are implied.) We also observe for the first time the decay $\tau^- \rightarrow \phi \pi^- \nu_\tau$, but it is treated here as a background process, together with the kinematically allowed but phase-space suppressed decays $\tau^- \rightarrow \phi \pi^- (n\pi) \nu_\tau$ ($1 \leq n \leq 4$). The result is based on a data sample of 401 fb^{-1} corresponding to 3.6×10^8 $\tau^+ \tau^-$ pairs collected near the $\Upsilon(4S)$ resonance with the Belle de-

* Corresponding author.

E-mail address: kenji@hepl.phys.nagoya-u.ac.jp (K. Inami).

tector at the KEKB asymmetric-energy e^+e^- (3.5 on 8 GeV) collider [5].

The Belle detector is a large-solid-angle magnetic spectrometer that consists of a silicon vertex detector, a 50-layer central drift chamber, an array of aerogel threshold Čerenkov counters, a barrel-like arrangement of time-of-flight scintillation counters, and an electromagnetic calorimeter comprised of CsI(Tl) crystals located inside a superconducting solenoid coil that provides a 1.5 T magnetic field. An iron flux-return located outside of the coil is instrumented to detect K_L^0 mesons and identify muons. The detector is described in detail elsewhere [6]. Two inner detector configurations were used. A 2.0 cm radius beampipe and a 3-layer silicon vertex detector were used for the first sample of 158 fb^{-1} , while a 1.5 cm radius beampipe, a 4-layer silicon detector and a small-cell inner drift chamber were used to record the remaining 244 fb^{-1} [7].

2. Event selection

We look for $\tau^- \rightarrow \phi K^- \nu_\tau$ candidates in the reaction $e^+e^- \rightarrow \tau^+\tau^-$ with the following signature:

$$\tau_{\text{signal}}^- \rightarrow \phi + K^- + (\text{missing})$$

$$\hookrightarrow K^+ K^-,$$

$$\tau_{\text{tag}}^+ \rightarrow (\mu/e)^+ + n(\leq 1)\gamma + (\text{missing}),$$

where ‘missing’ denotes other possible daughters not reconstructed. The detection of ϕ mesons relies on the $\phi \rightarrow K^+K^-$ decay ($\mathcal{B} = (49.2 \pm 0.6)\%$ [1]); the final evaluation of the signal yield is carried out using the K^+K^- invariant mass distribution.

The selection criteria described below are determined from studies of Monte Carlo (MC) simulated events. The background samples consist of $\tau^+\tau^-$ (1570 fb^{-1} , which does not include any decay mode with a ϕ meson) and $q\bar{q}$ continuum, $B^0\bar{B}^0$, B^+B^- and two-photon processes. For signal, we generate samples with 2×10^6 $\tau^- \rightarrow \phi K^- \nu_\tau$, $\phi K^- \pi^0 \nu_\tau$, $\phi \pi^- \nu_\tau$ and $\phi \pi^- \pi^0 \nu_\tau$ events.

The transverse momentum for a charged track is required to be larger than $0.06 \text{ GeV}/c$ in the barrel region ($-0.6235 < \cos\theta < 0.8332$, where θ is the polar angle relative to the direction opposite to that of the incident e^+ beam in the laboratory frame) and $0.1 \text{ GeV}/c$ in the endcap region ($-0.8660 < \cos\theta < -0.6235$, and $0.8332 < \cos\theta < 0.9563$). The energy of photon candidates is required to be larger than 0.1 GeV in both regions.

To select a τ -pair sample, we require four charged tracks in an event with zero net charge, and a total energy of charged tracks and photons in the center-of-mass (CM) frame less than 11 GeV . We also require that the missing momentum in the laboratory frame be greater than $0.1 \text{ GeV}/c$, and that its direction be within the detector acceptance, where the missing momentum is defined as the difference between the momentum of the initial e^+e^- system, and the sum of the observed momentum vectors. The event is subdivided into 3-prong and 1-prong hemispheres according to the thrust axis in the CM frame. These are referred to as the signal and tag side, respectively. We allow at most one photon on the tag side to account

for initial state radiation, while requiring no extra photons on the signal side to reduce the $q\bar{q}$ backgrounds.

We require $\cos\theta_{\text{thrust-miss}}^{\text{CM}} < -0.6$ to reduce backgrounds from other τ decays and $q\bar{q}$ processes, where $\theta_{\text{thrust-miss}}^{\text{CM}}$ is the opening angle between the thrust axis (on the signal side) and the missing momentum in the CM frame. In order to remove the $q\bar{q}$ background, we require that the invariant mass of the particles on the tag side (if a γ is present) be less than $1.8 \text{ GeV}/c^2$ ($\simeq m_\tau$). Similarly, the effective mass of the signal side must be less than $1.8 \text{ GeV}/c^2$. Moreover, we require that the lepton likelihood ratio $P_{\mu/e}$ be greater than 0.1 for the charged track on the tag side. Here P_x is the likelihood ratio for a charged particle of type x ($x = \mu, e, K$ or π), defined as $P_x = L_x / (\sum_x L_x)$, where L_x is the likelihood for particle type hypothesis x , determined from responses of the relevant detectors [8]. The efficiencies for muon and electron identification are 92% for momenta larger than $1.0 \text{ GeV}/c$ and 94% for momenta larger than $0.5 \text{ GeV}/c$, respectively.

We require that both kaon daughters of the ϕ candidate have kaon likelihood ratios $P_K > 0.8$ and $\cos\theta > -0.6$. The kaon identification efficiency is 82%. To suppress combinatorial backgrounds from other τ decays and $q\bar{q}$ processes, we require that the ϕ momentum be greater than $1.5 \text{ GeV}/c$ in the CM frame. After these requirements, the remaining contributions from $B^0\bar{B}^0$, B^+B^- , Bhabha, μ pair and two-photon backgrounds are negligible.

To separate $\phi K^- \nu_\tau$ from $\phi \pi^- \nu_\tau$, the remaining charged track is required to satisfy the same kaon identification criteria as the ϕ daughters. The $\tau^+\tau^-$ and $q\bar{q}$ backgrounds are reduced by requiring that the opening angle ($\theta_{\phi K}^{\text{CM}}$) between the ϕ and K^- in the CM frame satisfy $\cos\theta_{\phi K}^{\text{CM}} > 0.92$, and that the CM momentum of the ϕK^- system be greater than $3.5 \text{ GeV}/c$. For $\phi \pi^- \nu_\tau$, we require that the charged track be identified as a pion, $P_\pi > 0.8$, and that the opening angle between the ϕ and π^- in the CM frame satisfy $\cos\theta_{\phi\pi}^{\text{CM}} < 0.98$. This last requirement suppresses the background from $\tau^- \rightarrow \phi K^- \nu_\tau$ and $\tau^- \rightarrow \phi K^- \pi^0 \nu_\tau$.

Fig. 2(a) shows the K^+K^- invariant mass distribution after all $\tau^- \rightarrow \phi K^- \nu_\tau$ selection requirements. As there are two possible K^+K^- combinations from the $K^-K^+K^-$ tracks on the signal side, this distribution has two entries per event. Therefore, the signal MC shape includes a long tail due to the wrong K^+K^- combination. Non-resonant backgrounds arise mainly from $\tau^- \rightarrow K^+K^- \pi^- \nu_\tau$, which has a branching fraction of $\mathcal{B} = (1.53 \pm 0.10) \times 10^{-3}$ [1]. Small contributions are expected from $q\bar{q}$ processes as described below.

3. Signal and background evaluation

The detection efficiencies ϵ for $\tau^- \rightarrow \phi K^- \nu_\tau$ and the cross-feed rates from $\phi K^- \pi^0 \nu_\tau$ and $\phi \pi^- \nu_\tau$ are evaluated, as listed in Table 1, from MC simulation using KKMC [9], where the $V-A$ interaction is assumed at the vertices and the final hadrons decay according to non-resonant phase space. The efficiencies include the branching fraction for $\phi \rightarrow K^+K^-$.

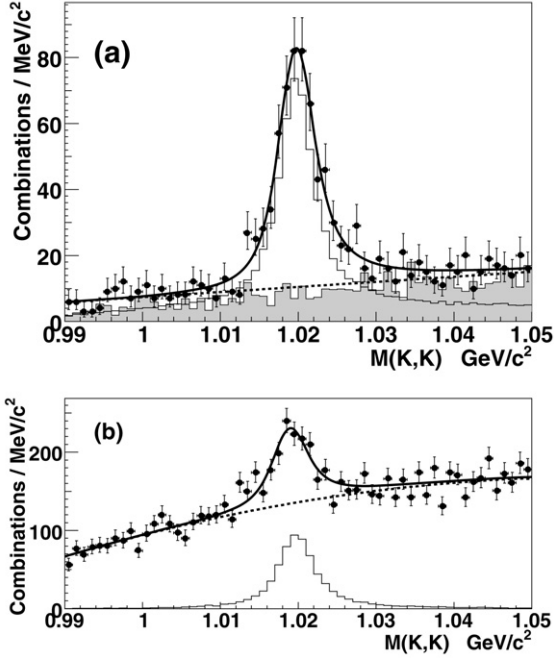


Fig. 2. K^+K^- invariant mass distributions for (a) $\tau^- \rightarrow \phi K^- \nu_\tau$ and (b) $\tau^- \rightarrow \phi \pi^- \nu_\tau$. Points with error bars indicate the data. The shaded histograms show the expectations from $\tau^+\tau^-$ and $q\bar{q}$ background MC simulations. The open histogram is the signal MC with $\mathcal{B}(\tau^- \rightarrow \phi K^- \nu_\tau) = 4 \times 10^{-5}$ in (a) and $\mathcal{B}(\tau^- \rightarrow \phi \pi^- \nu_\tau) = 6 \times 10^{-5}$ in (b). The curves show the best fit results, and the dashed curves indicate the non-resonant background contributions. See the text for details.

Table 1
Detection efficiencies ϵ and cross-feed rates (%), from MC simulation. The errors are from the MC statistics

Candidates	Decay modes		
	$\phi K \nu$	$\phi \pi \nu$	$\phi K \pi^0 \nu$
$\tau \rightarrow \phi K \nu$	1.826 ± 0.009	0.049 ± 0.002	0.328 ± 0.006
$\tau \rightarrow \phi \pi \nu$	0.110 ± 0.002	1.663 ± 0.014	0.009 ± 0.001

The signal yields are extracted by a fit to the K^+K^- invariant mass distribution. For signal, we use a p -wave Breit–Wigner (BW) distribution convolved with a Gaussian function (of width σ) to account for the detector resolution. The ϕ width is fixed to be $\Gamma_\phi = 4.26 \text{ MeV}/c^2$ [1] but σ is allowed to float. First- and second-order polynomial background functions are used for $\tau^- \rightarrow \phi K^- \nu_\tau$ and $\phi \pi^- \nu_\tau$ decays, respectively. The fit results are also shown in Fig. 2. The obtained signal yields are $N_{\phi K \nu} = 573 \pm 32$ and $N_{\phi \pi \nu} = 753 \pm 84$. The σ 's from the fits are $1.2 \pm 0.3 \text{ MeV}/c^2$ and $1.2 \pm 0.7 \text{ MeV}/c^2$ for $\phi K^- \nu_\tau$ and $\phi \pi^- \nu_\tau$, respectively, which are consistent with MC simulation.

MC studies show that only the $\tau^- \rightarrow \phi \pi^- \nu_\tau$, $\tau^- \rightarrow \phi K^- \pi^0 \nu_\tau$ and $q\bar{q}$ samples yield significant contributions peaking at the ϕ mass. The contributions of other backgrounds are less than 0.01% and can be neglected. The contribution of $\tau^- \rightarrow \phi \pi^- \nu_\tau$ events to the $\phi K^- \nu_\tau$ sample is estimated using $N_{\phi \pi \nu}$ and the misidentification rate, as discussed below. Other contributions are estimated as follows.

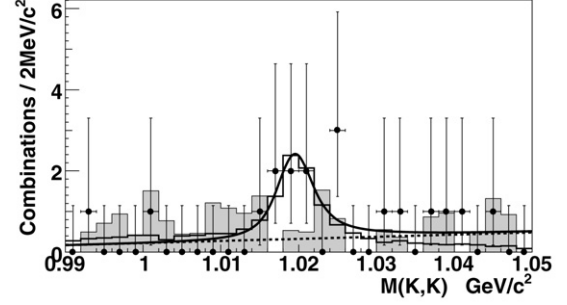


Fig. 3. K^+K^- invariant mass distributions for $\tau^- \rightarrow \phi K^- \pi^0 \nu_\tau$. Points with error bars indicate the data. Histograms show the MC expectations of τ -pairs (shaded) and signal (open) with a branching fraction of 3×10^{-6} . The solid curve shows the best fit result and the dashed curve shows the non-resonant background contribution.

To evaluate the branching fraction and background contribution from $\tau^- \rightarrow \phi K^- \pi^0 \nu_\tau$, we select $\pi^0 \rightarrow \gamma\gamma$ candidates and combine them with $\phi K^- \nu_\tau$ combinations that satisfy the requirements listed above. The signal yield is estimated by fitting the resulting K^+K^- invariant mass distribution with a p -wave BW distribution plus a linear background function, as shown in Fig. 3. The resulting yield is $8.2 \pm 3.8 \phi K \pi^0 \nu$ events. Using a detection efficiency $\epsilon_{\phi K \pi^0 \nu} = (0.396 \pm 0.007)\%$ obtained from MC simulation, and an $e^+e^- \rightarrow \tau^+\tau^-$ sample normalization $N_{\tau\tau} = 401 \text{ fb}^{-1} \times 0.892 \text{ nb} = 3.58 \times 10^8$, we obtain a branching fraction $\mathcal{B}(\tau^- \rightarrow \phi K^- \pi^0 \nu_\tau) = (2.9 \pm 1.3) \times 10^{-6}$. However, this must be corrected for the unknown contamination of $\tau^- \rightarrow \phi \pi^- \pi^0 (n\pi) \nu_\tau$ ($0 \leq n \leq 3$) decays. Using this value, we estimate the $\tau^- \rightarrow \phi K^- \pi^0 \nu_\tau$ background in the $\tau^- \rightarrow \phi K^- \nu_\tau$ sample to be $N_{\phi K \pi^0 \nu} = (6.8 \pm 3.1)$ events, given a cross-feed rate for $\tau^- \rightarrow \phi K^- \pi^0 \nu_\tau$ to the $\tau^- \rightarrow \phi K^- \nu_\tau$ sample of $(0.328 \pm 0.006)\%$ (see Table 1).

From a MC study, we find a $q\bar{q}$ contamination of $N_{q\bar{q}} = 6.6 \pm 2.5$. To take into account the uncertainty in ϕ production in the $q\bar{q}$ MC, we compare MC results with enriched $q\bar{q}$ data by demanding that the effective mass of the tag side be larger than $1.8 \text{ GeV}/c^2$. With this selection, the background is $q\bar{q}$ dominated and the other backgrounds are negligible. The yield in data is 262 ± 21 events, and the yield in the $q\bar{q}$ MC is 117 ± 10 events. We subsequently scale the above $q\bar{q}$ background estimate by the ratio $f = 2.23 \pm 0.26$; the result is $N_{q\bar{q}} = 14.8 \pm 5.8$ events.

4. Results

The peaking backgrounds described above, $\tau^- \rightarrow \phi K^- \pi^0 \nu_\tau$ and $q\bar{q}$, are subtracted from the signal yield, leaving $N_{\phi K \nu} = (573 \pm 32) - (6.8 \pm 3.1) - (14.8 \pm 5.8) = 551 \pm 33$ events. To take into account cross-feed between $\tau^- \rightarrow \phi K^- \nu_\tau$ and $\tau^- \rightarrow \phi \pi^- \nu_\tau$ due to particle misidentification ($K \leftrightarrow \pi$), we solve the following simultaneous equations:

$$N_{\phi K \nu} = 2N_{\tau\tau} (\epsilon_{\phi K \nu} \times \mathcal{B}_{\phi K \nu} + \epsilon_{\phi \pi \nu}^{\phi K \nu} \times \mathcal{B}_{\phi \pi \nu}), \quad (1)$$

$$N_{\phi \pi \nu} = 2N_{\tau\tau} (\epsilon_{\phi K \nu}^{\phi \pi \nu} \times \mathcal{B}_{\phi K \nu} + \epsilon_{\phi \pi \nu} \times \mathcal{B}_{\phi \pi \nu}), \quad (2)$$

where $\mathcal{B}_{\phi K\nu}$ and $\mathcal{B}_{\phi\pi\nu}$ are the branching fractions for $\tau^- \rightarrow \phi K^- \nu_\tau$ and $\tau^- \rightarrow \phi\pi^- \nu_\tau$, respectively. The detection efficiencies, ϵ 's, are listed in Table 1. The factor $\epsilon_{\phi K\nu}^{\phi\pi\nu}$ is the efficiency for reconstructing $\tau^- \rightarrow \phi K^- \nu_\tau$ as $\tau^- \rightarrow \phi\pi^- \nu_\tau$ while $\epsilon_{\phi\pi\nu}^{\phi K\nu}$ is the efficiency for reconstructing $\tau^- \rightarrow \phi\pi^- \nu_\tau$ as $\tau^- \rightarrow \phi K^- \nu_\tau$. The resulting branching fraction for $\tau^- \rightarrow \phi K^- \nu_\tau$ is

$$\mathcal{B}_{\phi K\nu} = (4.05 \pm 0.25) \times 10^{-5}, \quad (3)$$

where the uncertainty is due to the statistical uncertainty in the $N_{\phi K\nu}$ and $N_{\phi\pi\nu}$ terms. The uncertainty in the detection efficiencies, ϵ 's, will be taken into account in the systematic error. The result for $\mathcal{B}_{\phi\pi\nu}$ is $\mathcal{B}_{\phi\pi\nu} = (6.05 \pm 0.71) \times 10^{-5}$; however, small background from $\tau^- \rightarrow \phi\pi^-(n\pi)\nu_\tau$ ($1 \leq n \leq 4$) decays is included and must be subtracted to obtain the final branching fraction.

The systematic uncertainties are estimated as follows: the uncertainties in the integrated luminosity, $\tau^+\tau^-$ cross-section and trigger efficiency are 1.4%, 1.3% and 1.1%, respectively. Track finding efficiency has an uncertainty of 4.0%. Uncertainties in lepton and kaon identification efficiencies and fake rate are evaluated, respectively, to be 3.2% and 3.1% by averaging the estimated uncertainties depending on momentum and polar angle of each charged track. To evaluate the systematic uncertainty of fixing Γ_ϕ in the BW fit, we calculate the change in the signal yield when Γ_ϕ is varied by ± 0.05 MeV/ c^2 (the uncertainty quoted by the PDG) [1]: the result is 0.2%. The branching fraction for $\phi \rightarrow K^+K^-$ gives an uncertainty of 1.2% [1]. The signal detection efficiency $\epsilon_{\phi K\nu}$ has an uncertainty of 0.5% due to MC statistics. A total systematic uncertainty of 6.5% is obtained by adding all uncertainties in quadrature. The resulting branching fraction is then

$$\mathcal{B}(\tau^- \rightarrow \phi K^- \nu_\tau) = (4.05 \pm 0.25 \pm 0.26) \times 10^{-5}. \quad (4)$$

Finally, we consider the possibility that a resonant state contributes to the final ϕK^- hadronic system. We generate a resonant MC with the KKMC simulation program. The weak current is generated with a $V - A$ form while the ϕK^- system is assumed to be produced from a 2-body decay of a resonance. In Fig. 4(a), the ϕK^- mass distribution for data is compared to MC; the combinatorial background is subtracted using the K^+K^- sideband. The MC distributions correspond to $(M, \Gamma) = (1650, 100)$ MeV/ c^2 , $(M, \Gamma) = (1570, 150)$ MeV/ c^2 , and also non-resonant phase space. Fig. 4(b) shows the ϕ 's angular distribution in the ϕK^- rest frame ($\cos\alpha$), where the negative of the lab frame direction in the ϕK^- frame is taken as the reference axis. It indicates an isotropic distribution in the ϕK^- system. For both the invariant mass and angular distributions of the ϕK^- system, the phase space MC reproduces the signal distribution well. We therefore neglect systematic uncertainty due to possible resonant structure. On the other hand, the 1650 MeV/ c^2 state assumed in the CLEO search [4], indicated by the dotted histogram in Fig. 4(a), clearly cannot account for the entire signal. If production via a single resonance is assumed, the best agreement with data is found for a mass and a width of $\simeq 1570$ MeV/ c^2 and $\simeq 150$ MeV/ c^2 , respectively, as shown

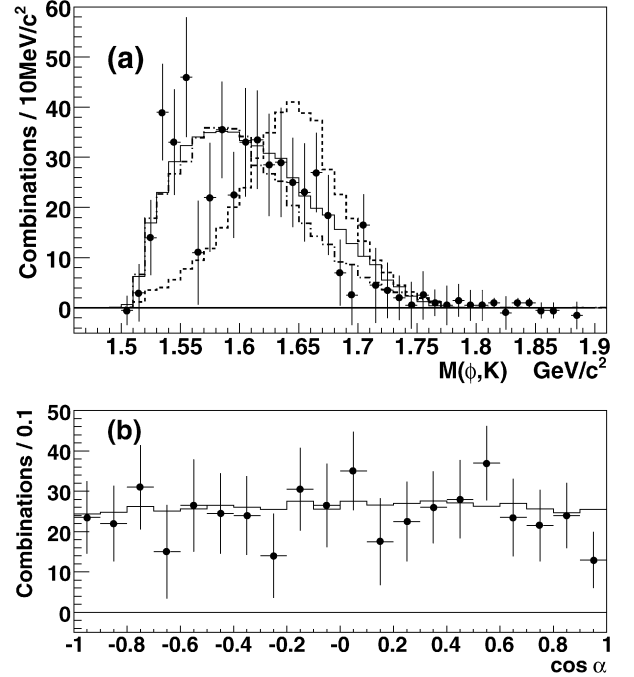


Fig. 4. (a) Invariant mass and (b) angular distributions for the ϕK^- system. The non- ϕ -resonant backgrounds are subtracted using the sideband spectra. Points with error bars indicate the data. The open histogram shows the phase-space-distributed signal MC, and dotted and dot-dashed histograms indicate the signal MC mediated by a resonance with $M = 1650$ MeV/ c^2 and $\Gamma = 100$ MeV/ c^2 and $M = 1570$ MeV/ c^2 and $\Gamma = 150$ MeV/ c^2 , respectively. In the MC, a branching fraction of 4×10^{-5} is assumed. (b) ϕ 's angular distribution in the ϕK^- rest frame, where the negative of the lab frame direction in the ϕK^- frame is taken as the reference axis.

by the dot-dashed histogram. However, since the shape of the resonant MC is similar to the phase-space-distributed MC, we cannot draw any strong conclusions about an intermediate resonance with $\Gamma \sim O(100$ MeV/ c^2) in this narrow mass range of ~ 250 MeV/ c^2 .

5. Conclusion

Using 401 fb^{-1} of data, we make the first observation of the rare decay $\tau^- \rightarrow \phi K^- \nu_\tau$. The measured branching fraction is

$$\mathcal{B}(\tau^- \rightarrow \phi K^- \nu_\tau) = (4.05 \pm 0.25 \pm 0.26) \times 10^{-5}. \quad (5)$$

Acknowledgements

We gratefully acknowledge the essential contributions of Mari Kitayabu, which are described in her bachelor thesis at Nagoya University. We thank the KEKB group for the excellent operation of the accelerator, the KEK cryogenics group for the efficient operation of the solenoid, and the KEK computer group and the National Institute of Informatics for valuable computing and Super-SINET network support. We acknowledge support from the Ministry of Education, Culture, Sports, Science, and Technology of Japan and the Japan Society for the Promotion of Science; the Australian Research Council and the Australian Department of Education, Science and Training;

the National Science Foundation of China and the Knowledge Innovation Program of the Chinese Academy of Sciences under contract No. 10575109 and IHEP-U-503; the Department of Science and Technology of India; the BK21 program of the Ministry of Education of Korea, the CHEP SRC program and Basic Research program (grant No. R01-2005-000-10089-0) of the Korea Science and Engineering Foundation, and the Pure Basic Research Group program of the Korea Research Foundation; the Polish State Committee for Scientific Research; the Ministry of Science and Technology of the Russian Federation; the Slovenian Research Agency; the Swiss National Science Foundation; the National Science Council and the Ministry of Education of Taiwan; and the US Department of Energy.

References

- [1] Particle Data Group, W.-M. Yao, et al., *J. Phys. G* 33 (2006) 1.
- [2] G. López Castro, D.A. López Falcón, *Phys. Rev. D* 54 (1996) 4400.
- [3] S.I. Eidelman, V.N. Ivanchenko, *Nucl. Phys. B (Proc. Suppl.)* 55C (1997) 181.
- [4] CLEO Collaboration, P. Avery, et al., *Phys. Rev. D* 55 (1997) R1119.
- [5] S. Kurokawa, E. Kikutani, *Nucl. Instrum. Methods A* 499 (2003) 1, and other papers included in this volume.
- [6] Belle Collaboration, A. Abashian, et al., *Nucl. Instrum. Methods A* 479 (2002) 117.
- [7] Belle SVD2 Group, Y. Ushiroda, *Nucl. Instrum. Methods A* 511 (2003) 6.
- [8] K. Hanagaki, et al., *Nucl. Instrum. Methods A* 485 (2002) 490; A. Abashian, et al., *Nucl. Instrum. Methods A* 491 (2002) 69.
- [9] S. Jadach, B.F.L. Ward, Z. Wąs, *Comput. Phys. Commun.* 130 (2000) 260.